

# Simulation on dispersion and birefringence properties of photonic crystal fiber

Qiang Xu (许强)

Department of Physics and Information Technology, Baoji University of Arts & Science,  
Baoji 721016, PR China

Corresponding author: xuqiangwlx@163.com

Received December 14, 2014; accepted January 20, 2014; posted online March 25, 2014

Combination of full-vector finite element method with anisotropic perfectly matched layers results in a novel structure of low-dispersion photonic crystal fiber with high birefringence. The negative dispersion can be obtained at a wavelength of 1.55  $\mu\text{m}$  by adjusting the lattice constant  $\Lambda$  and the round air hole diameter  $d$ . Numerical results show that the dispersion variation is negative in the C band, the dispersion slope values are between 0.112 and 0.142  $\text{ps} \cdot \text{km}^{-1} \cdot \text{nm}^{-2}$  over the C band, and the birefringence is  $5.7 \times 10^{-3}$ .

OCIS codes: 130.5296, 060.5295, 060.2310.

doi: 10.3788/COL201412.S11302.

Photonic crystal fibers (PCFs)<sup>[1,2]</sup>, also called holey fibers (HFs) or microstructured fibers, are characterized by a periodic arrangement of air holes around a central high-index core along the entire length of the fiber. Control of chromatic dispersion in PCFs is a very important problem for practical applications in optical communication systems, dispersion compensation, and nonlinear optics. So far, various PCFs with remarkable dispersion properties, such as shifting of zero dispersion wavelengths to the visible and near-infrared wavelength, an ultra-flattened chromatic dispersion, and a large positive dispersion with a negative slope in the 1.55- $\mu\text{m}$  wavelength range, have been reported<sup>[3]</sup>. Fibers with flattened dispersion are mostly preferred for optical frequency conversion and broad-band flattened supercontinuum generation.

PCFs with high birefringence are of significant research interest, as they could be widely used in fiber sensors, in the long fiber loops of gyroscopes and high-bit-rate communication systems with long-term stabilized operation<sup>[4]</sup>. Modal birefringence in these PCFs has been predicted to have values an order magnitude of  $10^{-3}$  higher than that of the conventional HB fibers ( $10^{-4}$ )<sup>[5]</sup>. To our knowledge, the key point in realizing the birefringence is to destroy the symmetry of the fiber structure and increase the effective index difference between the two orthogonal polarization modes<sup>[6]</sup>. According to previous researches, highly birefringent PCFs can be obtained by breaking the circular symmetry implementing asymmetric defect structures such as dissimilar air hole diameters along the two orthogonal axes<sup>[7,8]</sup>, asymmetric core design<sup>[9,10]</sup> and by replacing the circular holes with elliptical ones in the cladding<sup>[11,12]</sup> and squeezed hexagonal lattice PCFs<sup>[13]</sup>. Another kind of highly birefringent structure reported is a square lattice PCF<sup>[14]</sup>. According to the symmetry theory, the rectangular lattice is potentially more anisotropic than the triangular and honeycomb lattices<sup>[14,15]</sup>.

The design of a simple PCF structure with low dispersion and high birefringence characteristics is an ongoing challenge. Taking all the above circumstances into account, in this paper, we propose a novel PCF, in which the fiber includes a solid silica core and a cladding with rectangular lattice elliptical air holes along the fiber length. The design is validated using an efficient full-vector finite-element method (FV-FEM) with anisotropic perfectly matched layers (PMLs) for accurate modeling of PCFs<sup>[3,16]</sup>.

As shown in Fig. 1, the structure of PCF studied here has a transverse section consisting of four elliptical air holes. The whole fiber is based on pure silica, and all air holes are arranged by using square lattice structure along the fiber length, and a central air hole is eliminated to form a light propagation region. It is characterized by the lattice constant  $\Lambda$ , the elliptical air hole major axis  $a$  and minor axis  $b$ , and the round air hole diameter  $d$ . It is defined as  $\eta = b/a$ . In our work, the refractive index of the air hole is  $n_0 = 1$ , and the refractive index of the silica background is  $n = 1.45$ .

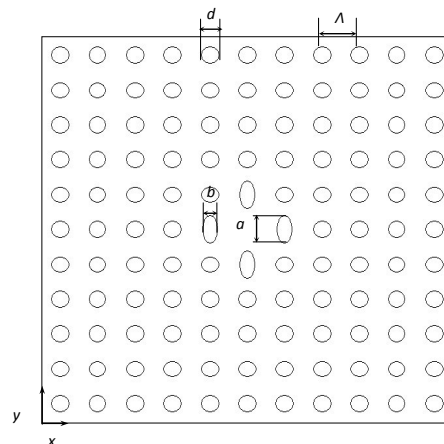


Fig. 1. Schematic cross-section of the proposed PCF structure.

The cross-section of the PCF is divided into homogeneous subspaces, where we employ the FEM to solve Maxwell's equations by accounting for the adjacent subspaces<sup>[3,16]</sup>. Following vector wave equation is derived from Maxwell's equations by employing anisotropic PMLs<sup>[3,16]</sup>

$$\nabla \times ([s]^{-1} \nabla \times \vec{E}) - k_0^2 n^2 [s] \vec{E} = 0, \quad (1)$$

where  $k_0 = 2\pi/\lambda$  is the free-space wave number,  $\lambda$  being the wavelength,  $\vec{E}$  denotes the electric field,  $n$  is the refractive index,  $[s]$  is the PML matrix, and  $[s]^{-1}$  is an inverse matrix of  $[s]$ .

Waveguide dispersion of optical fibers is a major factor causing optical pulse spreading. Once the modal effective indexes  $n_{eff}$  are solved, the waveguide dispersion parameter  $D_w(\lambda)$  can be obtained<sup>[17]</sup>

$$D_w(\lambda) = -\frac{\lambda}{c} \frac{\partial^2 \text{Re}(n_{eff})}{\partial \lambda^2}, \quad (2)$$

where  $c$  is the velocity of the light in a vacuum,  $\lambda$  is the wavelength of the light. Our design procedure is based on the possibility to approximate the real dispersion  $D(\lambda)$  by a sum of the waveguide dispersion (or geometrical dispersion)  $D_w(\lambda)$  and the material dispersion  $D_m(\lambda)$ <sup>[18]</sup>

$$D(\lambda) \approx D_w(\lambda) + D_m(\lambda). \quad (3)$$

The material dispersion can be obtained directly from the three-term Sellmeier formula, while the waveguide dispersion can be calculated as in Eq. (2). In order to obtain total dispersion, from Eq. (3), if we are able to design the PCF in such a way that it can exhibit a waveguide dispersion nearly opposite to that of the material dispersion, namely  $D_w(\lambda) \approx -D_m(\lambda)$  over a finite number of frequencies<sup>[19]</sup>, we can partially fulfill the nearly-zero dispersion requirement.

The dependences of  $D_w(\lambda)$  are plotted on various incremental values of the design parameter of the proposed PCF, as in Fig. 2. Figure 2(a) shows the  $D_w(\lambda)$  curves by fixing  $\eta = 0.5$  and  $d = 0.7 \mu\text{m}$ , while changing  $\Lambda$  from 1.2 to 1.4  $\mu\text{m}$  in step size 0.1  $\mu\text{m}$ . It can be seen from Fig. 2(a) that the proposed PCF has a negative dispersion parameter and a negative dispersion slope in the wavelength range around 1.55  $\mu\text{m}$ , which demonstrates an excellent dispersion

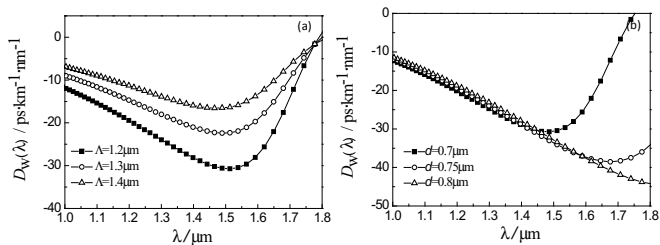


Fig. 2. Waveguide dispersion  $D_w(\lambda)$  curves as a function of the wavelength  $\lambda$  for various incremental values of the design parameters  $\Lambda$ ,  $d$ , and  $\eta$ . (a) Change  $\Lambda$  when  $d = 0.7$  and  $\eta = 0.5$   $\mu\text{m}$ . (b) Change  $d$  when  $\Lambda = 1.2$   $\mu\text{m}$  and  $\eta = 0.5$ .

compensating property. The value of  $D_w(\lambda)$  decreases gradually with wavelength in a shorter wavelength, and increases gradually in a longer wavelength range, owing to the fact that the air hole function decreases with an increase in  $\Lambda$ . Meanwhile, the minimum dispersion wavelength has a blue shift with an increase in  $\Lambda$ . The  $D_w(\lambda)$  decreases gradually with the wavelength as well as shows up-shift with the increase in  $\Lambda$ . Here, in order to obtain better dispersion compensating, we have fixed  $\Lambda$  at 1.2  $\mu\text{m}$ .

In addition, Fig. 2(b) shows the  $D_w(\lambda)$  curves by changing  $d$  from 0.7 to 0.8  $\mu\text{m}$  in step size 0.05  $\mu\text{m}$  by fixing  $\Lambda$  at 1.2  $\mu\text{m}$  and  $\eta$  at 0.5. Figure 2(b) shows that the proposed PCF has a negative dispersion parameter and negative dispersion slope in the wavelength range around 1.55  $\mu\text{m}$ , and the value of  $D_w(\lambda)$  decreases gradually with wavelength, while the value of  $D_w(\lambda)$  increases with increase in  $d$ . Meanwhile, the minimum dispersion wavelength has a red shift with an increase in  $d$ . Analyzing Figs. 2(a) and (b), it is understood that the proposed PCF has optimal dispersion curves and better dispersion compensation when the fiber parameters are optimized as follows:  $\Lambda = 1.2$   $\mu\text{m}$ ,  $d = 0.7$   $\mu\text{m}$ , and  $\eta = 0.5$ .

The sum of the PCF can, thereby, be altered to obtain the total dispersion profile [Fig. 3(a)]. For convenience, the total dispersion is calculated using Eq. (3), but written in a slightly different form as follows:

$$D(\lambda) \approx D_w(\lambda) - (-D_m(\lambda)). \quad (4)$$

In Fig. 3(a), the curves corresponding to the  $D_w(\lambda)$ , the sign-changed  $-D_m(\lambda)$ , and  $D(\lambda)$ , are represented in triangular sign, square sign and black circle sign, respectively. According to Eq. (4), the black circle curve corresponding to  $D(\lambda)$  is obtained by subtracting the values of the square curve from the triangular one. As it can be observed, the total dispersion is  $-7.04 \text{ ps} \cdot \text{km}^{-1} \cdot \text{nm}^{-1}$  at wavelength of 1.55  $\mu\text{m}$ , and the dispersion slope values are between 0.112 and 0.142  $\text{ps} \cdot \text{km}^{-1} \cdot \text{nm}^{-2}$  over the C band, as shown in Fig. 3(b).

Birefringence is defined as a difference between the real part of effective refractive indices of  $x$  and  $y$  polarized fundamental modes and can be expressed as<sup>[20]</sup>

$$B(\lambda) = \left| \text{Re}(n_{eff}^y(\lambda)) - \text{Re}(n_{eff}^x(\lambda)) \right|. \quad (8)$$

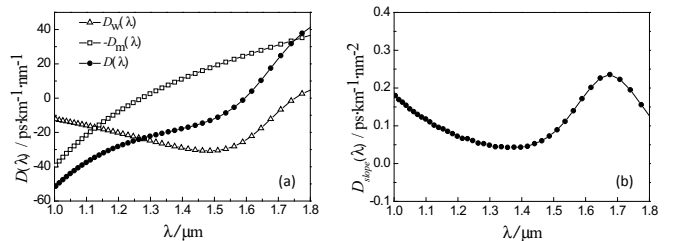


Fig. 3. (a) Curves for  $D_w(\lambda)$ ,  $D_m(\lambda)$ , and  $D(\lambda)$  versus wavelength for the optimized PCF when  $\Lambda = 1.2$   $\mu\text{m}$ ,  $d = 0.7$   $\mu\text{m}$ , and  $\eta = 0.5$ . (b)  $D_{Slope}(\lambda)$  versus wavelength for the optimized PCF when  $\Lambda = 1.2$   $\mu\text{m}$ ,  $d = 0.7$   $\mu\text{m}$ , and  $\eta = 0.5$ .

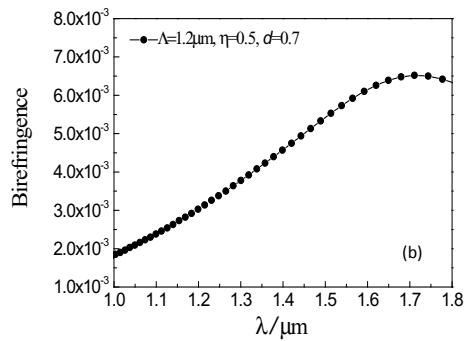


Fig. 4. Birefringence curves as a function of the wavelength  $\lambda$  for the proposed PCF with optimized design parameters  $A = 1.2 \mu\text{m}$ ,  $d = 0.7 \mu\text{m}$ , and  $\eta = 0.5$ .

where,  $n_{eff}^x$  and  $n_{eff}^y$  are effective refractive indices of two orthogonal polarization fundamental modes.

In Fig. 4, the calculated fundamental mode birefringence as a function of the wavelength  $\lambda$  has been plotted, for the optimized design parameters. It can be observed that the birefringence is about  $5.7 \times 10^{-3}$  at the wavelength of  $1.55 \mu\text{m}$ .

In addition, from the electric field distribution of the fundamental mode in Fig. 5 at the wavelength of  $\lambda = 1.55 \mu\text{m}$ , we can observe the strong confinement of light in the core of the PCF.

We demonstrate a novel-type low-dispersion PCF with high birefringence. By tuning the pitch and hole size, it is demonstrated how the dispersion of the fiber can be designed and fibers with positive as well as near-zero dispersion slope are fabricated. When the parameters of the proposed PCF are optimized to be  $A = 1.2 \mu\text{m}$ ,  $d = 0.7 \mu\text{m}$ , and  $\eta = 0.5$ , the dispersion slope values are between  $0.112$  and  $0.142 \text{ ps} \cdot \text{km}^{-1} \cdot \text{nm}^{-2}$  over the C band, and the birefringence is  $5.7 \times 10^{-3}$  at  $1.55 \mu\text{m}$ .

The work was supported by the Baoji University of Arts and Science Key Research Foundation (No. ZK14011).

## References

1. J. C. Knight, *Nature* **424**, 847 (2003).
2. P. Russell, *Science* **299**, 358 (2003).
3. K. Saitoh, M. Koshiba, T. Hasegawa, and E. Sasaoka, *Opt. Express* **11**, 843 (2003).

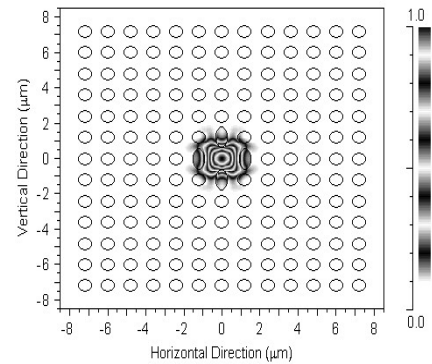


Fig. 5. Normalized electric field distribution of the x-polarized mode at a wavelength of  $\lambda = 1.55 \mu\text{m}$  for the proposed PCF.

4. X. L. Tan, Y. F. Geng, and J. Zhou, *Opt. Laser Technol.* **43**, 1331 (2011).
5. J. Liang, M. J. Yun, W. J. Kong, X. Sun, W. F. Zhang, and S. X. Xi, *Optik*, **122**, 2151 (2011).
6. H. Ademgil and S. Haxha, *J. Lightwave Technol.* **26**, 441 (2008).
7. A. Ortigosa-Blanch, J. C. Knight, W. J. Wadsworth, J. Arriaga, B. J. Mangan, T. A. Birks, and P. S. J. Russell, *Opt. Lett.* **25**, 1325 (2000).
8. J. Ju, W. Jin, and M. S. Demokan, *IEEE Photon. Technol. Lett.* **15**, 1375 (2003).
9. T. P. Hansen, J. Broeng, S. E. B. Libori, E. Knuders, A. Bjarklev, J. R. Jensen, and H. Simonsen, *IEEE Photon. Technol. Lett.* **13**, 588 (2001).
10. S. Kim, C. S. Kee, J. Lee, Y. Jung, H. G. Choi, and K. Oh, *J. Appl. Phys.* **101**, 016101 (2007).
11. D. Chen and L. F. Shen, *IEEE Photonics Technol. Lett.* **19**, 185 (2007).
12. Z. Wu, D. X. Yang, L. Wang, L. Rao, L. Zhang, K. Chen, W. J. He, and S. Liu, *Opt. Laser Technol.* **42**, 387 (2010).
13. L. Zhang and C. Yang, *Opt. Express* **12**, 2371 (2004).
14. M. Y. Chen, R. J. Yu, and A. P. Zhao, *J. Opt. A: Pure Appl. Opt.* **6**, 997 (2004).
15. A. Ferrando and J. J. Miret, *Appl. Phys. Lett.* **78**, 3184 (2001).
16. K. Saitoh and M. Koshiba, *IEEE J. Quantum Electron.* **38**, 927 (2002).
17. K. Saitoh and M. Koshiba, *Opt. Express* **13**, 267 (2005).
18. S. Haxha and H. Ademgil, *Opt. Commun.* **281**, 278 (2008).
19. A. Ferrando, E. Silvestre, P. Andres, J. J. Miret, and M. V. Andres, *Opt. Express* **9**, 687 (2001).
20. Y. N. Zhang, L. Y. Ren, Y. K. Gong, X. H. Li, L. R. Wang, and C. D. Sun, *Appl. Opt.* **49**, 3208 (2010).